

Evaluation of viscous characteristics of Newtonian and non-Newtonian fluids by falling head flow tests with an ultrasonic velocity profiler

Ryou Obinata¹, Shun Nomura¹, Kazuo Tani¹, Minori Kyoj¹, Tomonori Ihara²

¹ Dep. of Marine Resources and Energy, Tokyo University of Marine Science and Technology, 4-5-7 Konan, Minato-ku, Tokyo 108-8477, Japan

² Dep. of Marine Electronics and Mechanical Engineering, Tokyo University of Marine Science and Technology, 2-1-6 Etchujima, Koto-ku, Tokyo 135-8533, Japan

The purpose of this study is to investigate the flow velocity profile in the pipe of falling head flow test (FHFT) with an ultrasonic velocity profiler (UVP). FHFT was proposed to evaluate the viscous characteristics of Bingham fluids. Its application was extended to varieties of non-Newtonian fluids. In the FHFT, the viscosity parameters such as the plastic viscosity and the yield stress can be derived by measuring the falling head process in the apparatus composed of the vertical and horizontal pipes. If the yield stress, $\tau_y > 0$, a plug flow is theoretically considered to develop in the central region of the flow. In the experiment, UVP was placed along the horizontal pipe to measure the velocity profile. Two FHFTs were conducted using Glycerin as the Newtonian fluid, and CMC solution as the non-Newtonian fluid, respectively. By the UVP measurement, a parabolic profile was observed in Glycerin, while a semi-parabolic profile representing a plug flow in the middle was observed in CMC solution. The velocity profiles postulated from the viscosity characteristics obtained by FHFT were consistent with those measured by UVP. Thus, this FHFT is applicable to evaluate the viscous characteristics of both Newtonian and non-Newtonian fluids.

Keywords: Flow test, Viscous characteristic, Viscosity measurement, Pipe flow

1. Introduction

Marine mineral resources such as polymetallic nodules exist on the seabed around Japan. To lift up ores of these mineral resources from the seabed to the sea surface, Tani et al. [1] proposed to use a viscous fluid with yield stress as a carrier material (CM). To study the lifting efficiency of the relevant systems, it is important to evaluate the viscous characteristics of CMs (i.e., the relationship between the shear stress, τ , and the shear rate, $\dot{\gamma}$). At present, rotational viscometers such as the B type viscometer are commonly used for viscosity measurements. However, they are not suitable for fluids containing sand particles and can only measure the apparent relationship between shear stress and shear rate for non-Newtonian fluids. To overcome these problems, Kyoj et al. [2] proposed the falling head flow test (FHFT) as a novel method to measure the viscosity characteristics of both Newtonian and non-Newtonian fluids.

In this study, FHFTs were conducted using Glycerin as a Newtonian fluid and CMC solution as a non-Newtonian fluid. The applicability of this test method was examined through the investigation of the flow velocity profile in the pipe of FHFT with an ultrasonic velocity profiler (UVP).

2. Method of Falling Head Flow Test

2.1 Principle of falling head flow test

Figure 1 shows the principle of FHFT and the laminar flow of a non-Newtonian fluid in the pipe. In this test, the fluid (density ρ) flows down in the pipe (radius R). This pipe is composed of the vertical and horizontal sections with the height, h , and the length, L , respectively. The viscous characteristics are obtained by optically analyzing the

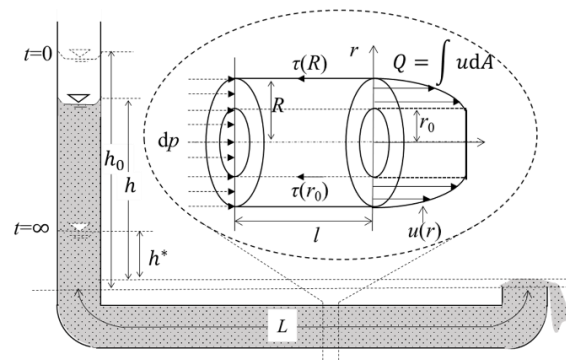


Figure 1: Principle of the falling head flow test.

change of the elevation difference, h , with time, t . The initial condition is set as $h = h_0$ at $t = 0$.

Eq.1 shows the equilibrium condition for the small section with the length, l , in the pipe. Eq.2 shows the relationship between the shear stress τ and the shear rate $\dot{\gamma}$ of a non-Newtonian fluid by Herschel-Bulkley model which express as shear thinning and yield stress effectively in the pipe where k is the consistency index, n is the flow index, and τ_y is the yield stress. Considering $dp = \rho gh$ and $l = L + h$, the mean velocity U was obtained as Eq.3 using the ratio of plug flow radius r_0 to R as Eq.4 from Eq.1 and Eq.2. Each parameter to present U can be defined from the test setting except k , n , and the terminal head loss, h^* , at $t = \infty$. τ_y is derived by Eq.5. Eq.6 defines the theoretical head loss $h_{the(t+dt)}$ at $t = t + dt$ with $U_{obs(t)}$ derived from $h_{obs(t)}$ obtained through FHFT. Then, as Eq.7, the appropriate combination of k , n and h^* are derived by minimizing the sum of the squares of the difference between $h_{obs(t)}$ and $h_{the(t)}$.

$$\pi r^2 dp = 2\pi r l \tau_{(r)} \quad (1)$$

$$\tau_{(r)} = \tau_y + k\dot{\gamma}_{(r)}^n \quad (2)$$

$$U = \frac{Q}{\pi R^2} \quad (3)$$

$$= \left(\frac{R\rho g}{2k} \frac{h}{L+h} \right)^{\frac{1}{n}} \frac{R}{1+\frac{1}{n}} \left(1 - \frac{r_0}{R} \right)^{1+\frac{1}{n}} \left\{ 1 - \frac{2}{2+\frac{1}{n}} \left(1 - \frac{r_0}{R} \right) + \frac{2}{\left(2 + \frac{1}{n} \right) \left(3 + \frac{1}{n} \right)} \left(1 - \frac{r_0}{R} \right)^2 \right\}$$

$$\frac{r_0}{R} = \left(\frac{h^*}{L+h^*} \right) \left(\frac{L+h}{h} \right) \quad (4)$$

$$\tau_y = \frac{\rho g h^*}{L+h^*} \quad (5)$$

$$h_{the(t+dt)} = h_{the(t)} - U_{obs(t)} dt \quad (6)$$

$$h_{(t=0)} = h_0$$

$$\sum_{t=0}^t \{ h_{obs(t)} - h_{the(t)}(k, n, h^*) \}^2 = \min. \quad (7)$$

2.2 Setting of FHFTS

Two kinds of fluids were used in FHFT; Glycerin (Glycerol $\geq 95.0\%$, Hayashi Pure Chemical Ind., Ltd) and CMC (Carboxymethyl Cellulose, CMC HP-80, Daicel Miraizu., Ltd) solution which was diluted with water to the mass concentration of 1.0%, respectively. In addition, to improve the visibility of the flow, food coloring (Food coloring red, KENIS Co., Ltd) was mixed with not higher than 0.01% solution mass.

Figure 2 shows the experimental apparatus. Table 1 shows the densities of fluids and the test conditions of the experimental apparatus. R was 20.4 mm. The initial heads, h_0 , and the length of the horizontal section, L , were determined so that the liquid level at the downstream end was quasi-static and stable. The temperature of fluids was from 20.0 °C to 21.0 °C. Here, h was measured from the recorded movie through the image analysis every 0.1 s for Glycerin and 1.0 s for CMC 1%, respectively.

Table 1: Condition of FHFT.

Fluid	ρ (Mg/m ³)	h_0 (m)	L (m)
Glycerin	1.220	0.879	2.360
CMC 1.0%	1.020	1.835	1.330

2.3 Setting of UVP

Figure 2 and Figure 3 show the experimental apparatus and concept of UVP measurement, respectively. A laboratory built UVP setup was used, which consists of a pulser/receiver, A/D converter and signal processing software. The UVP was fixed with the jig and installed in

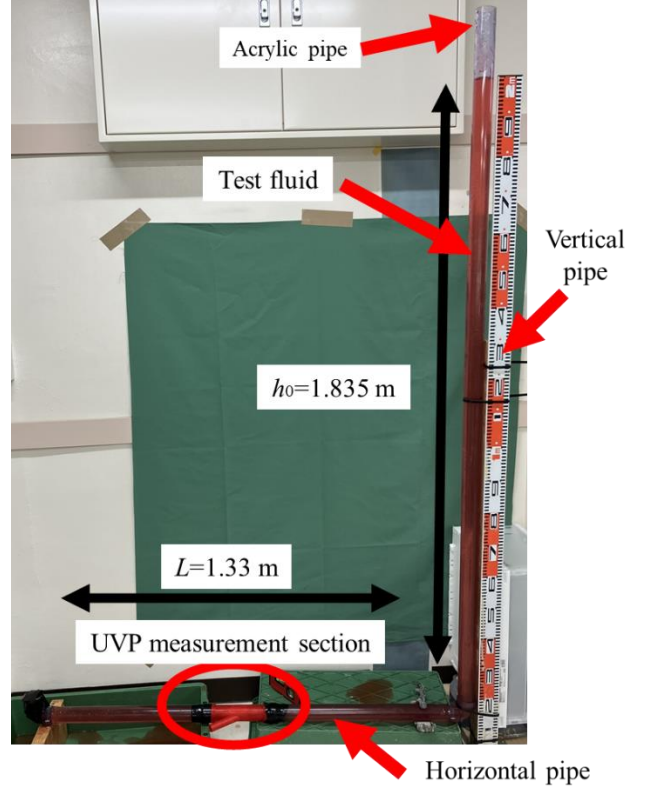


Figure 2: Experimental apparatus.

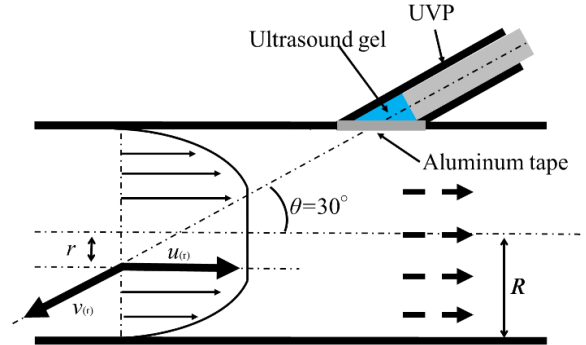


Figure 3: Concept of UVP measurement.

the middle section of the horizontal pipe. The inclination angle θ of ultrasound beam was set 30 degrees from the flow direction. The velocity profile $v_{(r)}$ in the ultrasonic beam direction is transformed into the flow direction $u_{(r)}$ by Eq.8. Table 2 shows the parameters of UVP measurement. The measurements were conducted with the transducer whose diameter is 16mm. The emitting frequency is 1 MHz.

$$u_{(r)} = - \frac{v_{(r)}}{\cos 30^\circ} \quad (8)$$

Table 2: Parameters of UVP measurement.

Parameters	Glycerin	CMC
Pulse repetition frequency PRF (Hz)	800	100
Sound velocity of the fluid (m/s)	2000	1710
Sampling rate (Hz)	10	5

3. Test Results and Discussions

Figure 4 shows $h-t$ relationships and mean velocities $U = dh/dt$ of Glycerin by FHFT at the representative points, G1: $t = 2.0$ s, G2: $t = 5.0$ s and G3: $t = 10.0$ s. Figure 5 shows those of CMC 1% at the representative points, C1: $t = 10$ s, C2: $t = 70$ s, C3: $t = 150$ s. In the case of Glycerin, the h falls down rapidly, $\Delta h > 0.7$ m for $t < 10$ s, whereas in CMC, it falls slowly even after $t = 1000$ s.

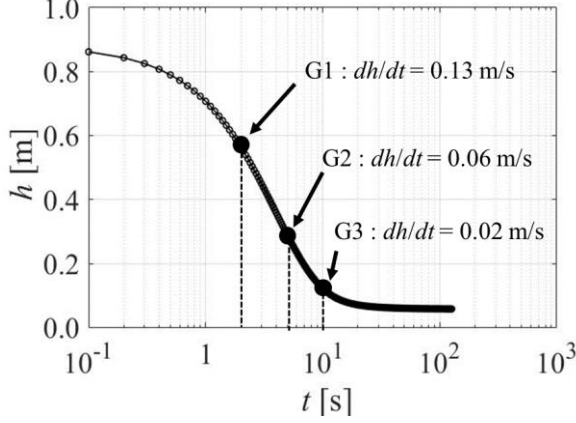


Figure 4: $h-t$ relationship and U of Glycerin at G1, G2, G3.

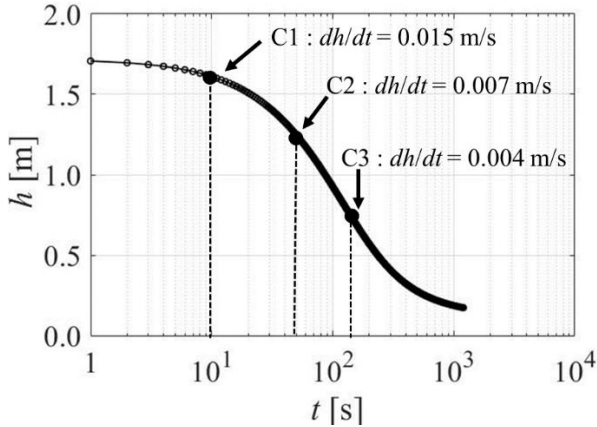


Figure 5: $h-t$ relationship and U of CMC 1% at C1, C2, C3.

Table 3 shows the viscosity parameters, k , n , and τ_y , measured by FHFT and B type viscometer (DV-II+pro-LV, Brookfield). It should be noted that τ_y could not be obtained by the B type viscometer, thereby shown as NA. In Herschel-Bulkley equation (Eq.2), it's well known that $n = 1$ and $\tau_y = 0$ for a Newtonian fluid such as Glycerin, and $n < 1$ for a pseudoplastic fluid such as CMC solution. It is found that the FHFT can evaluate reasonable values of n for both Newtonian and non-Newtonian fluids.

Using these parameters in Table 3, the velocity profiles were assumed by Eq.9 and Eq.10 as well by Benslimane A. et al. [3]. In the pipe, the laminar flow area ($\tau_{(r)} > \tau_y$) and the plug flow area ($0 < \tau_{(r)} \leq \tau_y$) are presented in Eq.9 and Eq.10, respectively. Figure 6 and Figure 7 show non-dimensional velocity profiles of Glycerin and CMC at the representative points, respectively. Those profiles were obtained according to the sampling rate in Table 2.

Table 3: Comparison of viscosity parameters by FHFT and B

Viscosity parameter	Glycerin		CMC 1%	
	FHFT	B type	FHFT	B type
k [Pa·s]	0.79	0.80	26	26
n [-]	1.0	1.2	0.44	0.29
τ_y [Pa]	3.1	NA	6.4	NA

$$u_{(r)} = \frac{R}{\tau_{(r)} k^{\frac{1}{n}} \frac{1}{n} + 1} \left\{ \begin{aligned} &(\tau_{(r)} > \tau_y) \\ &\left(\tau_{(r)} - \tau_y \right)^{\frac{1}{n}+1} \\ &- \left(\tau_{(r)} \frac{r}{R} - \tau_y \right)^{\frac{1}{n}+1} \end{aligned} \right\} \quad (9)$$

$$(0 < \tau_{(r)} \leq \tau_y) \quad (10)$$

$$u_{(r)} = \frac{R}{\tau_{(r)} k^{\frac{1}{n}} \frac{1}{n} + 1} \left(\tau_{(r)} - \tau_y \right)^{\frac{1}{n}+1}$$

In those figures, a comparison was made with the predicted profile by FHFT and the fitted profile for measured data by UVP using the least squares method with the range of $-1 \leq r/R \leq 0.7$ as assuming the velocity of 0 m/s on the pipe wall. From Figure 6, it was found that the profiles obtained by UVP of Glycerin present parabolic profiles and are consistent with the predicted profiles by FHFT for high and middle flow velocities (referring to G1 and G2). While, it is less consistent for the lowest flow velocity when the plug flow develops (referring to G3). This means that the dh/dt was larger than the predicted profiles by FHFT compared with G1 and G2. It suggests that the fluid was slipping on the pipe wall. At low velocities, the assumed boundary conditions at the pipe wall might be inconsistent due to fluid flow does not have enough shear stress for deformation at the pipe wall.

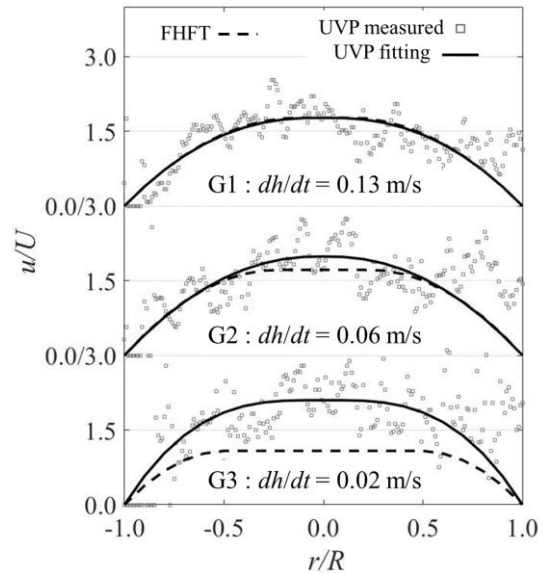


Figure 6: Velocity profiles of Glycerin at G1, G2, and G3.

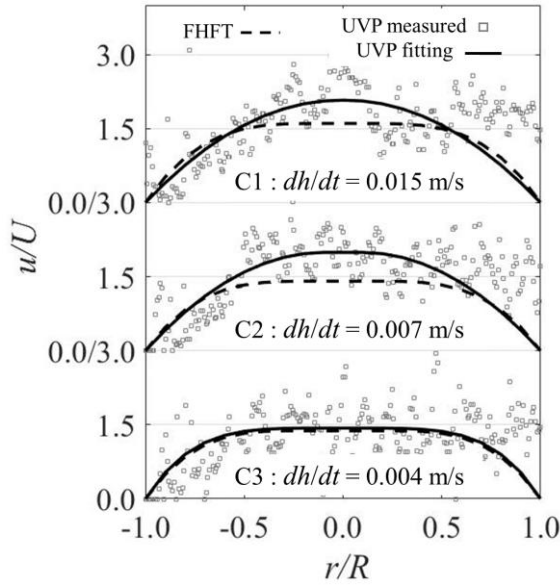


Figure 7: Velocity profiles of CMC 1% at C1, C2, and C3.

From Figure 7, it is concluded that the velocity profiles measured by both methods are consistent with each other. Those obtained by UVP show that the plug flow presents around the central region in the pipe (referring to C2 and C3). However, the difference between the measured profiles by UVP and the predicted profiles by FHFT is larger than that for Glycerin around $r/R = 0$. This is because CMC solutions have thickening structures made by polysaccharides in the fluid. As a result, it presents more non-linear characteristics to theoretical flow than Newtonian fluid.

Table 4: Comparison of viscosity parameters of Glycerin and CMC 1% by FHFT and UVP

Glycerin Viscosity parameter	FHFT	UVP		
		G1	G2	G3
k [Pa·s]	0.79	1.6	1.3	2.2
n [-]	1.00	0.81	0.91	0.55
τ_y [Pa]	3.1	1.0	0.4	0.4
CMC 1% Viscosity parameter	FHFT	UVP		
		C1	C2	C3
k [Pa·s]	26	18.1	25.5	28.0
n [-]	0.44	0.99	1.00	0.30
τ_y [Pa]	6.4	0.60	4.10	0.60

In Table 4, a comparison is made between the viscosity parameters obtained by FHFT and those obtained by UVP. For Glycerin, the parameters obtained by UVP exhibit Newtonian fluid characteristics at G1 and G2. Additionally, at C3, where the plug flow was most developed, the parameters obtained by UVP represent non-Newtonian fluid characteristics similar to those obtained by FHFT. However, the combination of n , k , and τ_y affect each other even the shape of the velocity profiles. As a result, it is found that a more appropriate method and reasonable solution to determine the parameter in Eq.2 is needed. Furthermore, influence of slip at the pipe wall may induce inconsistency of FHFT and UVP profile. Thereby, we need the confirmation of the boundary condition and more detailed observations near the pipe wall.

4. Conclusions

By FHFT, the viscosity parameters were measured of Glycerin and CMC 1% solutions, respectively. In these tests, velocity profiles in the pipe were measured using UVP at the same time to study the applicability of the FHFTs.

The results demonstrate that the velocity profiles derived from the viscosity parameters obtained through FHFT agreed well with those fitted from UVP measurement. Thus, it's justified to conclude that FHFT test is applicable to evaluate viscous characteristics of both Newtonian and non-Newtonian fluids.

References

- [1] Tani K., *et al.*: Method and devices for lifting valuable seafloor materials using carrier material, Japan Patent No. 6570000, (2018). (in Japanese)
- [2] Kyoji M., *et al.*: Falling head flow test to study pipe flow and viscous characteristics of carrier materials used for ore lifting from deep seafloor. ICPMG. pp.538-541, (2022).
- [3] Benslimane A., *et al.*: Laminar and turbulent pipe flow of bentonite solutions. Journal of Petroleum Science and Engineering, (2015).